Journal of Low Temperature Physics (2026) 222:40
https://doi.org/10.1007/s10909-026-03375-x

Recombination Rate of D Atoms in Solid D_2 in the Temperature Range from 0.23 to 1.64 K

C. K. Wetzel[1] · D. M. Lee[1] · S. Sheludiakov[2] · J. Ahokas[3] · S. Vasiliev[3] · V. V. Khmelenko[1]

Received: 23 October 2025 / Accepted: 22 January 2026

Abstract
The recombination rates of D atoms in solid D_2 films were measured in the temperature range 0.23–1.64 K. Atoms were formed in thin D_2 films by maintaining radio-frequency discharge above the film surface for several days. After stopping discharge the decay of D atoms concentrations was monitored at different temperatures by the method of electron spin resonance (ESR). Decreasing the films temperature from 1.64 to 0.23 K resulted in reducing the recombination rate from 7.2×10^{-26} cm^{3}s^{-1} to 1.0×10^{-27} cm^{3}s^{-1}.

Keywords Deuterium atoms · Solid Molecular deuterium · Electron spin resonance · Tunneling chemical reactions

1 Introduction

Solid molecular hydrogen isotopes (H_2, HD, D_2) are quantum solids characterized by small masses and weak intermolecular potentials. Light atomic impurities such as H and D atoms embedded in these solids are able to migrate from one lattice site to another by a repetition of the tunneling reactions [1–3],

$$H + H_2 \rightarrow H_2 + H \tag{1}$$

✉ C. K. Wetzel
wetzecam@tamu.edu

V. V. Khmelenko
khmel@tamu.edu

[1] Institute for Quantum Science and Engineering, Department of Physics and Astronomy, Texas A&M University, College Station, TX 77843, USA

[2] PsiQuantum, Palo Alto, CA 94304, USA

[3] Department of Physics and Astronomy, University of Turku, 20014 Turku, Finland

Published online: 09 February 2026

$$D + D_2 \rightarrow D_2 + D \tag{2}$$

When two atoms encounter each other at neighboring lattice sites they recombine. Exchange tunneling reactions also take place in the solid mixtures of molecular hydrogen isotopes [4–9]:

$$D + H_2 \rightarrow H + HD \tag{3}$$

$$D + HD \rightarrow H + D_2 \tag{4}$$

A substantial production of H atoms occurs due to reactions (3) and (4). Exchange reactions of hydrogen isotopes are the simplest and most fundamental among the chemical reactions. These reactions have been the subject of numerous theoretical and experimental studies [10–14]. These reactions are of special interest in the interstellar chemistry of the early universe and play an important role in the dynamics of deuterium in the primordial gas [15–17]. Measurements of the reactions (1, 2, 3 and 4) in solids at low temperatures make it possible to study them at very low energies, whereas gas-phase experiments utilizing molecular beams are restricted to much higher energies [18, 19]. Since two-body recombination of H or D atoms is inhibited by conservation laws, recombination in the interstellar environment must occur on surfaces or within solids. It has been suggested that grains of solid H_2 could persist in the interstellar medium [20]. Therefore, studies of tunneling and recombination processes in cryocrystals are also relevant to astrochemistry, as they shed light on mechanisms that may also occur in space [21, 22]. It is therefore interesting to study the isotope effects on the exchange chemical reactions. For this, studies of the recombination rates of H atoms in H_2 solids and D atoms in D_2 solids should be compared.

Investigations of the recombination rates of H atoms in solid H_2 were performed in the temperature range from 0.1 to 6 K [23–27]. It was found that at temperatures above 4.3 K the recombination rate of H atoms in solid H_2 follows the Arrhenius law, $k_r \sim \exp(-E_a/k_BT)$, where $E_a \sim 103$ K and k_B is the Boltzmann constant [23, 24]. However, at temperatures between 1.3 and 4.2 K, the rate constant is linearly dependent on temperature $k_r \sim AT$, where $A = (2 \pm 1) \times 10^{-24}\,\mathrm{cm^3 s^{-1} K^{-1}}$ [14, 23]. Moreover, at even lower temperatures, in the range 0.1–−0.9 K the recombination rate becomes much smaller, for example, at $T = 300$ mK, $k_r = 1.5 \times 10^{-25}\,\mathrm{cm^3 s^{-1}}$ and shows practically absence of recombination at the lowest temperature under study, $T = 100$ mK [25–27].

The studies of the recombination of D atoms in D_2 solids were performed over the temperature range 1.9–−9.5 K [3, 9, 24]. Similar to the case for the H in H_2 system, at $T \geq 7.5$ K, the recombination of D atoms in normal D_2 solids obey the Arrhenius law $k_D \sim \exp(-E_a/k_BT)$, but the value of $E_a = 270 \pm 30$ K [24], is larger than for H in H_2. In the temperature range 4.2-−7.5 K the recombination of D atoms proceeds due to quantum diffusion initiated by two-phonon process and follows the formula $k_D = BT^9$ [24]. There were also measurements of recombination rate of D atoms in D_2 at lower temperatures. Measurements at $T = 1.9$ K and

$T = 4.2$ K provided almost identical values for $k_D = 3.2 \times 10^{-27}$ cm^{3}s^{-1} [2], and measurement at $T = 0.15$ K gave a value $k_D = 3(2) \times 10^{-28}$ cm^{3}s^{-1} [9].

All mentioned above measurements of the recombination rates of H(D) atoms in molecular solids were performed by method of electron spin resonance (ESR). The decrease in atom concentrations in time was monitored while the temperature of the solid samples of molecular hydrogen isotopes was stabilized at different values. However, additional factors can also influence the observed recombination rates. In experiments with H atoms in solid H_2, the recombination rate measured upon running radio-frequency (RF) discharge above the molecular solid film was ~ 5 times larger than that measured after stopping discharge and stabilizing the same temperature $T = 0.7$ K [28]. This experiment points out the possible role of a fluxes of electrons and phonons on the recombination rates of atoms in molecular films.

In this work we studied the recombination of D atoms in solid normal D_2 films, over the temperature range 0.23-−1.64 K, by using a 128 GHz cryogenic ESR spectrometer [29]. All measurements were carried out by the traditional method of observing the decay of D atoms concentration in time at different temperatures. It was found that increasing temperature from 0.23 to 1.64 K resulted in increasing the D atom recombination rate from $1.0(8) \times 10^{-27}$ cm^{3}s^{-1} to $7.2(3.1) \times 10^{-26}$ cm^{3}s^{-1}.

2 Experimental Setup

The experimental setup is based on a commercial Oxford 200 dilution refrigerator, which accommodates a sample cell (SC) [29, 30] (see Fig. 1) and a cryogenic 128 GHz ESR spectrometer [31]. The sample cell is attached to the refrigerator mixing chamber and located in the center of a 4.6 T superconducting magnet. The ESR Fabry–Pérot resonator consists of an upper hemispherical mirror made of silver plated copper, and the bottom flat mirror. The flat mirror consists of a 1 cm^2 400-nm-thick gold layer deposited on a quartz crystalline disk. This quartz disk with deposited gold layers on both flat surfaces serves as a quartz microbalance (QM) for measurements of the D_2 film thicknesses deposited on the flat ESR mirror [29]. An RF coil placed near the QM (HNMR in Fig. 1) was used to run a RF discharge in a helium vapor, to create D atoms in the solid D_2 films.

A special chamber, the dissociator (H2S in Fig. 1) [29] where molecular hydrogen H_2 was condensed prior to the D_2 film deposition in the sample cell, was anchored to the continuous heat exchanger of the dilution refrigerator. By running discharge in the dissociator a steady flux of gas-phase H atoms was supplied into the sample cell. The electrons of hydrogen atoms in the gas phase are strongly polarized in high magnetic field (4.6 T) and at the low temperature of the experiment (0.6 K), resulting in formation of spin-polarized hydrogen gas (H↓) in the sample cell. The ESR lines of the H↓ were used for determination of the precise positions of the ESR signals of D(H) atoms in the solid D_2 films, and for calibration of the absolute numbers of D(H) atoms in the solid molecular deuterium films. The calibration principle was based on finding a correspondence between the heat released due to recombination of the gas-phase H↓ atoms and the decrease in area of their ESR lines [27, 28].

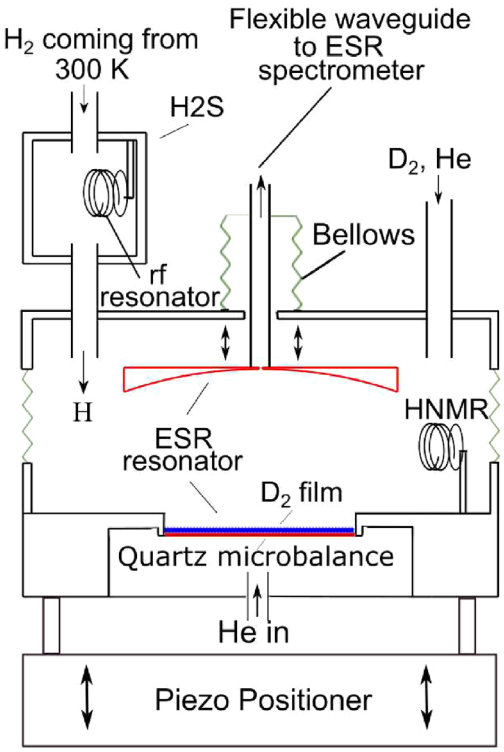

Fig. 1 Simplified schematic of the sample cell. H2S coil used for dissociation of H_2 molecules, HNMR coil tuned to the NMR resonance frequency of H atoms and for running RF discharge in the sample cell

We also analyzed the concentration-dependent broadening of the ESR lines of D(H) atoms in solid D_2 to evaluate the local concentration of D atoms embedded in the molecular deuterium films [27].

In this work, we studied two as deposited polycrystalline solid D_2 films. For deposition of D_2 films we used normal D_2 gas (67% J=0 ortho-D_2, 33% J=1 para-D_2 [32]) purchased from Cambridge Isotope Laboratories, Inc., which contained 0.4% HD impurity. The D(H) in D_2 samples were prepared by first condensing a solid D_2 film, from a room temperature reservoir through an electrically heated capillary, onto the flat mirror of the mm-wave Fabry–Pérot ESR cavity, which was also a Quartz Microbalance electrode (see Fig. 1). During the deposition of the film, the QM was maintained at a temperature of ≈ 1.5 K. By monitoring the change in resonance frequency of the quartz microbalance, the deposition rate and overall thickness of the D_2 films were measured to be ≈ 2 monolayer/s, and 1 μm, respectively. Natural para–ortho conversion of D_2 molecules in solid D_2 at low temperature is very slow ($0.06\%\text{hr}^{-1}$); therefore, we consider that the ortho–para content of the films did not change substantially over the duration of the experiment. After depositing the D_2 films the sample cell was evacuated, then a small amount of ^{4}He gas was condensed in the sample cell. A helical resonator located adjacent to the Fabry–Pérot cavity in the sample cell (HNMR in Fig. 1) was then driven with high-power radio-frequency (RF) pulses, which produced electric discharge in the volume of the sample cell. Free electrons produced in the discharge possessed an estimated energy of ~ 100

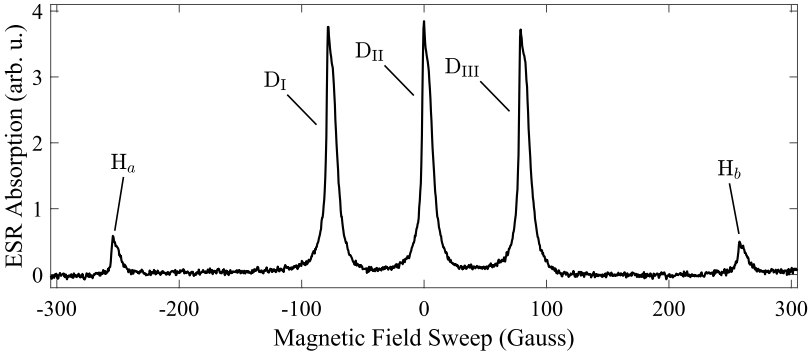

Fig. 2 Electron spin resonance (ESR) spectra of H and D atoms in the solid D_2 film recorded after 12 days of accumulation, at temperature $T = 580$ mK, and at magnetic field $B_0 = 4.6$ T

eV penetrated the surface of the D_2 films to an approximate depth of 100 nm. These electrons then produced D atoms within the film by dissociation of the constituent D_2 molecules ($D_2 + h\nu_e \rightarrow 2D$). Constant average RF discharge power was applied, while the sample temperature was stabilized using a feedback loop, over the course of days as the D atom content in the D_2 films saturated. The presence of stabilized atoms influences the para–ortho conversion of D_2 molecules in the vicinity of the atoms, but the concentrations of the atoms were less than 0.25% which does not significantly change the para–ortho content in the D_2 films.

The appearance of H atoms in the sample was due the presence of a known 0.4% impurity of HD in the D_2 gas used to form the films. The tunneling exchange reaction, $D + HD \rightarrow H + D_2$, was the primary mechanism for forming H atoms in the D_2 films [6, 8, 9]. Since the reverse reaction is endothermic with an activation energy $\epsilon_a/k_b \approx 500$ K, greatly exceeded the available thermal energy in the experiments $T \approx 600$ mK, the H atoms in the samples were considered to be immobile.

3 Experimental Results

3.1 ESR Spectra of H and D Atoms in the Solid D_2 film

After depositing the ~1 μm D_2 film on the flat mirror of Fabry–Pérot resonator, a small amount of ^{4}He was condensed in the SC, then RF discharge was started in the sample cell. The RF discharge was then maintained for ≈12 days, which produced D and H atoms in the film, by dissociation of D_2 and impurity HD molecules in the solid D_2 film, due to free electrons from the RF-discharge penetrating the film and interacting with the constituent molecules. The process of accumulation of D and H atoms in the solid D_2 film was monitored by ESR measurements. The majority of D and H atoms were produced in a thin layer near the surface the film due to the finite penetration depth, ≈ 100 nm of the electrons with average energy ≈ 100 eV produced by discharge. Figure 2 shows ESR spectra of D and H atoms taken at the end of the 12$^{\text{th}}$ day of accumulation. Due to the very small amount of (0.4%) impurity HD in

the solid D_2, the majority of atoms produced by dissociation were D atoms. However, throughout the experiment the observed ratio of [H]/([H] + [D]) was much greater ($\lessapprox 10\%$) than one would expect when considering only the dissociation of HD molecules. Indeed, the larger concentration of H atoms was accounted for by the the irreversible tunneling exchange reaction (4) which increased the observed H atom content in the film. The strong triplet of D atoms (D_I, D_{II}, D_{III}) and the weak doublet of H atoms (H_a, H_b) are seen in Fig. 2.

Additionally, it was observed that each of the components of the D and H spectra were asymmetric, and best fit as the sum of two Lorentzian lines. Figure 3 shows, in larger scale, the center field component of the D atom spectra (D_{II}) and the corresponding fit with two Lorentzian lines, the narrow C_1 line and the broad C_2 line. The two distinct components arise due to the finite penetration depth of the RF electrons into the film and diffusion of D atoms from the high concentration layer deeper into the D_2 film, similar to that of H atoms in solid H_2 films [28]. The broad component C_2 of the D(H) atom ESR spectra corresponds to the atoms in the region with high concentration of atoms near the film surface. The narrow C_1 component of D(H) atom ESR spectra corresponds to the atoms in the region with low concentrations. The high concentrations of D atoms were formed in the volume of D_2 film exposed to electrons from the discharge. The low concentration of D atoms found in the volume of D_2 film at the larger distances from the film surface where D atoms propagate due to spatial diffusion. At the end of accumulation the linewidth of the broad line, $\Gamma_{FWHM}(C_2)$, was equal to 10 G and the linewidth of the narrow line, $\Gamma_{FWHM}(C_1)$ was equal to 2.5 G. The C_1 component did not change during the time interval used for measurements of D atom concentration decay.

The local concentrations of D atoms in the D_2 films were determined from the FWHM line widths of the observed ESR lines, according equation:

$$\Gamma_{FWHM} = \gamma_{d\text{-}d}\, n_D + \Gamma_0 \tag{5}$$

where Γ_{FWHM} is the measured ESR FWHM linewidth, n_D is the local concentration of D atoms, $\gamma_{d\text{-}d} = 0.85 \times 10^{-19}\,\mathrm{G \cdot cm^3}$ is the dipole–dipole broadening coefficient

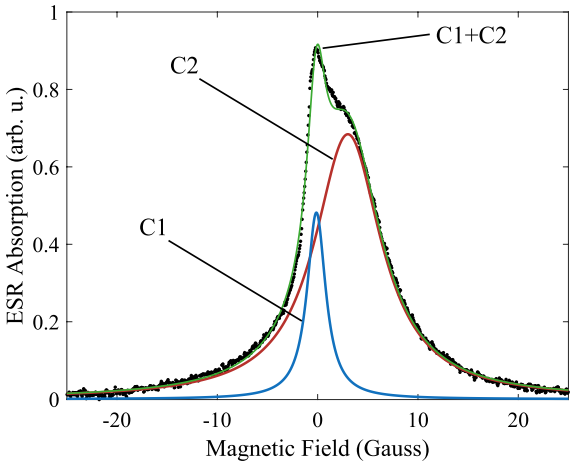

Fig. 3 Example fit of D atom center field ESR line (D_{II}) recorded during the recombination measurement at T=1.2 K. Measured Absorption signal (black circles), narrow component C1 (blue curve), broad component C2 (red curve), best fit sum of components C1+C2 (green curve)

determined from simulations [27], and $\Gamma_0 = 2.1$ G is the ESR broadening attributed to the nuclear moments of the surrounding D_2 molecules [33].

Since the concentrations of H atoms in the film were considerably smaller than the concentration of D atoms ($\sim 10\%$), the observed broadening of the H atoms ESR lines were predominantly due to dipole–dipole interactions with neighboring D atoms. Therefore, in calculating the local concentration of H atoms, the local concentrations of H atoms obtained from the ESR linewidth of H atoms were reduced by the ratio of the integral areas of ESR signals of H and D atoms.

3.2 Measurements of Recombination Rates of D Atoms in Solid D_2 Film

Measurements of the temperature dependence of the recombination rate of D atoms in the solid D_2 film were performed after stopping the accumulation of atoms in the D_2 film by turning off RF discharge. During these measurements the temperature of the SC was stabilized at different values, and the decay of D atom concentrations was recorded by the ESR method. In the following measurements of the recombination rates, we consider only the contribution from the broad, high concentration component C_2, since the narrow component C_1 exhibited no significant time dependence in both FWHM linewidth as well as integral area. Figure 4 shows dependence of reciprocal D atom concentration on time for different temperatures. Observation of the linearity of the data in Fig. 4 provides evidence that the D atom concentration decay process follows to the second order of D atoms recombination.

In the absence of RF discharge, and neglecting spatial diffusion of D atoms into the low concentration region of the film, the recombination of D atoms should follow second order recombination:

$$\frac{d}{dt}[\mathrm{D}] = -2k_r(T)[\mathrm{D}]^2 \tag{6}$$

which can be solved by integration giving the equation for the time dependence of the concentration of D atoms in the film as:

$$\frac{1}{[\mathrm{D}]} = \frac{1}{[\mathrm{D}]_0} + 2k_r(T)t \tag{7}$$

where [D] is the instantaneous concentration of D atoms in the film, $[\mathrm{D}]_0$ the concentration of D atoms at the beginning of each measurement, and $k_r(T)$ the temperature-dependent rate constant for the recombination reaction of D atoms. The results of the analysis of the data are collected in the Table 1. Table 1 shows temperatures, initial concentrations of D atoms, time intervals and recombination rates obtained in these measurements. The results are also shown in Fig. 5 as red triangles. It was found that increasing temperature from 0.23 K to 1.64 K resulted in growing recombination rate of D atoms in solid D_2 film from $2.3(8) \times 10^{-27}\,\mathrm{cm^3 s^{-1}}$ to $7.3(3.1) \times 10^{-26}\,\mathrm{cm^3 s^{-1}}$.

The measurements at 1.22 K and 1.30 K were performed on two separately prepared samples, with different film thicknesses and preparation conditions. The measurement at 1.22 K was performed in a 1 μm film of D_2 deposited at the rate 2 monolayer/s,

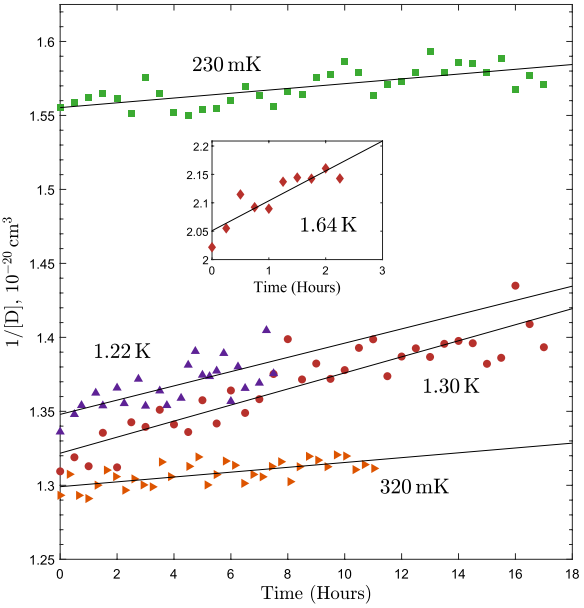

Fig. 4 Dependence of reciprocal concentration of D atoms on time at different temperatures: 230 mK—green squares, 320 mK—brown triangles, 1.22 K—blue triangles, 1.30 K—red circles, 1.64 K—red rhombs (in insert)

whereas the measurement at 1.30 K was performed in a thicker, $\sim 6\,\mu$m, film deposited at a faster rate ≈ 12 monolayer/s. Additionally, the D atoms were accumulated in the films at different temperatures, 580 mK for the 1 μm film, and 650 mK for the 6 μm. Despite different conditions for sample preparation, we observed similar crystalline line widths (~ 2.1 G) and saturation concentration of D atoms ($\sim 9 \times 10^{19}$ cm^{-3}) between the two samples. Each D_2 film was stored at temperature T < 1 K for a similar period of time before performing the recombination measurements reported in this work; therefore, we expect similar para–ortho D_2 content in both films. Furthermore, when we performed the recombination measurements at similar temperature and initial concentrations, the results between the differently prepared samples were in excellent agreement with each other, suggesting good reproducibility of these results.

The appearance of H atom signal in these experiments occurs due to the exchange tunneling reactions (4). The exchange reactions provided an additional channel for decreasing concentration of D atoms in the D_2 film, and affected the calculated according Eq.(7) recombination rates of D atoms. Therefore, as a next step, we consider the

Table 1 Temperatures of measurements, recombination rates of D atoms in D_2 matrix, initial concentrations of D atoms and time intervals of measurements

T, K	k_r, cm^{3}s^{-1}	$[D]_{initial}$, atoms cm^{-3}	$\Delta t_{measured}$, hours	k_r-corr, cm^{3}s^{-1}
0.23(1)	$2.3(8)\times10^{-27}$	6.43×10^{19}	17.0	$1.0(8)\times10^{-27}$
0.32(1)	$2.3(9)\times10^{-27}$	7.69×10^{19}	11.0	$1.2(9)\times10^{-27}$
1.22(2)	$7(2)\times10^{-27}$	7.42×10^{19}	7.5	$5.6(2)\times10^{-27}$
1.30(1)	$7.5(1.2)\times10^{-27}$	7.56×10^{19}	17.0	$6.5(1.2)\times10^{-27}$
1.64(5)	$7(3)\times10^{-26}$	4.88×10^{19}	2.5	$7.2(3.1)\times10^{-26}$

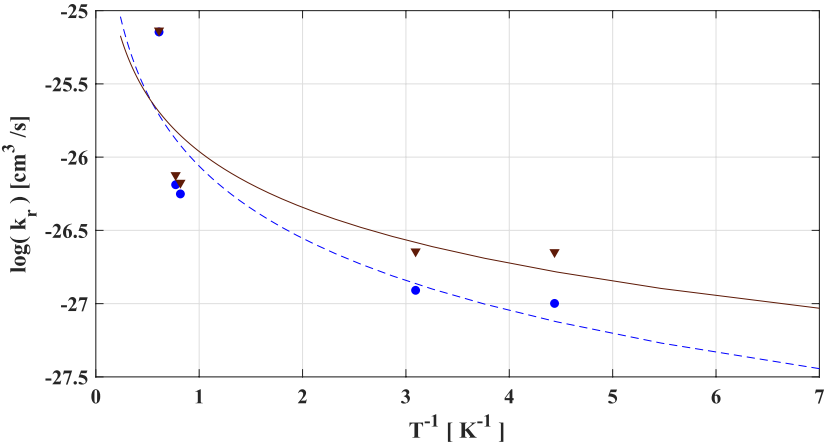

Fig. 5 Temperature dependence of the recombination rate constant for deuterium atoms in D_2 films. The results obtained by using Eq.(7) are shown by red triangles. The results including the correction for the exchange tunneling reaction (4) obtained following Eq.(9) are shown by blue circles. The sets of data before/after correction were fit by the equation $k_r(T) = BT^n$ and plotted here: before correction—solid red curve; best fit after correction—dashed blue curve

influence of the exchange tunneling reaction on the analysis of the data. We model the time dependence of the D atom concentration in the D_2 film by the following equation which includes exchange tunneling reaction:

$$\frac{d}{dt}[\mathrm{D}] = -k_{ex}[\mathrm{HD}][\mathrm{D}] - 2k_r(T)\,[\mathrm{D}]^2 \tag{8}$$

where [HD] is the concentration of HD molecules in the film and k_{ex} is the rate constant for the tunneling exchange reaction (4). Equation 8, may be solved exactly, giving the time dependence of the concentration of D atoms in the D_2 film as:

$$[\mathrm{D}](t) = \frac{[\mathrm{D}]_0}{\left(\frac{2k_r[\mathrm{D}]_0}{k_{ex}[\mathrm{HD}]} + 1\right)e^{k_{ex}[\mathrm{HD}]t} - \frac{2k_r[\mathrm{D}]_0}{k_{ex}[\mathrm{HD}]}} \tag{9}$$

In these experiments the total concentration of HD molecules in the film, was estimated to be $[\mathrm{HD}] \approx \left[\mathrm{D}_2\right] \times 0.4\% \approx 1.23 \times 10^{20}\,\mathrm{cm}^{-3}$ [34] nearly a factor of two larger than the maximum observed concentration of D atoms. Since the observed concentration of H atoms was $[\mathrm{H}] \leq [\mathrm{D}]/10$, we have treated the concentration of HD molecules as effectively constant for these analysis. Additionally, the rate constant for the exchange tunneling reaction was measured previously to be $k_{ex} = 9(4) \times 10^{-28}\mathrm{cm}^3\mathrm{s}^{-1}$ and was independent of temperature over the temperature range studied here [9]. The results for the corrected values of the D atoms recombination rates obtained from Eq. 9 are shown in the last column of Table 1, and as blue circles in Fig. 5.

4 Discussion

In the previous work the recombination of D atoms in solid D_2 were performed at temperatures higher than 1.9 K [2, 24, 35] and at only one lower temperature, equal to $T = 0.15$ K [9]. At temperature 0.15 K studies were performed in solid D_2 samples containing 0.23% HD molecules. The reported value of the rate constant of D atom recombination was corrected on the presence of the exchange tunneling reaction (4) taking place in this sample [9]. In this work we have studied the recombination rate of D atoms in solid molecular D_2 in the temperatures range from 0.23 K to 1.64 K. These results allow us to compare our measurements at the higher temperatures with the earlier measurements of other research groups. Additionally, the obtained results allow comparisons of the behavior of D in D_2 solids with that of H atoms in H_2 solids in the studied temperature range.

Figure 5 shows recombination rates obtained from Eq. 7 without considering corrections on proceeding exchange reaction (4) in the D_2 film. The fit obtained by the power law $k_r(T) = BT^n$ is optimal for values $\log(B) = -26.0$ and $n = 1.27$. When we used the same power law to fit the data obtained from Eq. 9, which includes the influence of exchange reaction (4), the optimal values $\log(B) = -26.1$, $n = 1.64$ were obtained. These fits are represented by the solid and dashed lines in Fig. 5. As shown in Fig. 5, the corrections are increasing with decreasing temperature. At temperatures above 1 K, the exchange reaction does not strongly influence the measurements of D atom recombination.

Figure 6a shows a comparison of the dependence of recombination rates on reciprocal temperature for H atoms in solid H_2 and D atoms in solid D_2 in the temperature range 0.14–10 K. Figure 6b shows the data only over the temperature range 1–10 K, to emphasize the high temperature range of the data. Both systems exhibit transition from a high-temperature regime for which recombination rate is governed by classical diffusion according equation $k_r \sim \exp(-E_a/k_B T)$ to a low-temperature regime which is determined by quantum diffusion at temperatures below, 4 K for H in solid H_2 and 7.5 K for D atoms in solid D_2 [24] (see Fig. 6b). The transition temperatures between different regimes for H in H_2 and D in D_2 are indicated by arrows in Fig. 6b. Therefore, we carried our investigations in the temperature range corresponding to quantum regime of D atom recombination. Takayanagi and Sato calculated reaction rates for isotopes of H atoms in molecular hydrogens utilizing theory based on gas-phase reactions [12]. Since the effect of the solid matrix was not included, good agreement with experiments was not expected, and their primary goal was to determine the temperature and isotope dependence of the reactions [13]. They calculated the tunneling exchange reaction rates assuming that recombination is limited by the approach (tunneling) of atoms. The ratio $k_r(H)/k_r(D)$ should reflect the isotope difference. According to their calculations the D recombination rate in D_2 should in fact be 10^5 times lower than that for H in H_2. However, in the experiments of Iskovskikh et al. [24] and in the present work, the ratio $k_r(H)/k_r(D)$ was in the range 100–1000, at least two orders of magnitude lower than was predicted. Hancock et al. applied similar theory, but only considered H and D in H_2 and HD [11]. Therefore, we suggest that the theory describing recombination rates for isotopes of H atoms in solid molecular hydrogens should be revised, with emphasis on

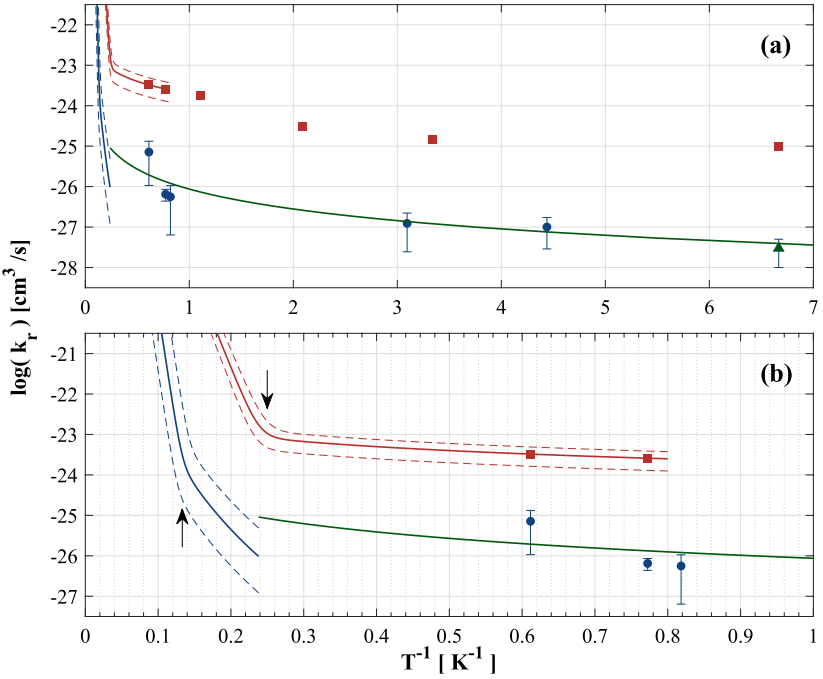

Fig. 6 Comparison of recombination rate constants measured in this work with previous results **a** in temperature range 0.14–10 K, **b** in temperature range 1–10 K for better demonstration of the transition from classical diffusion (at high temperatures) to quantum diffusion (at low temperatures). Temperature dependence of recombination rate constant of D atoms in solid D_2 obtained in this work (blue circles), from [9] (blue triangle), and from [24] (blue curve). The recombination rate of H atoms in solid H_2 from [24] (red curve), and from [25, 35] (red squares). Dashed curves represent the errors for data obtained in [24]. The transition temperatures for H atoms in solid H_2 and D atoms in D_2 are indicated by arrows. Green curve represents the best fit of the data (blue circles) according to the equation $k_r(T) = BT^n$

accounting for solid matrix and the isotope effects observed experimentally. Our results show that recombination of D atoms in solid D_2 occur much faster than that predicted theoretically. The theory should include a process of para–ortho conversion of D_2 molecules in the vicinity of D atoms. The para–ortho conversion generates phonons in the solid D_2 film, which can accelerate the D atom recombination.

All results presented in this work were obtained after stopping RF discharge in the sample cell. However, in the previous work on studying recombination and spatial diffusion of H atoms in H_2 films the influence of fluxes of electrons and phonons as well as the concentration of ortho-H_2 on the recombination rates and spatial diffusion of H atoms was established [28, 36]. In future work we plan investigations of the influences of the fluxes of electrons and phonons and the concentration of para-D_2 on the recombination rates and spatial diffusion of D atoms in D_2 films at temperatures below 1 K.

5 Conclusion

1. The recombination rates of D atoms in solid D_2 films were measured in the temperature range from 0.23 to 1.64 K.
2. It was found that the presence of 0.4% impurity HD molecules in the D_2 films influenced the measurements of the recombination rates of D atoms at temperatures below 1 K. The exchange tunneling reactions of D atoms with HD molecules should be accounted for in the analysis of the experimental data, especially for the lowest temperatures.
3. Temperature dependence of the recombination rate of D atoms in solid D_2 follows the power law $k_r(T) \sim BT^n$, where $\log(B) = -26.1$, $n = 1.64$.
4. Decreasing temperature from 1.64 to 0.23 K led to reducing D atom recombination rate from 7.2×10^{-26} to 1.0×10^{-27} $cm^3 s^{-1}$

Author Contributions C.K.W and V.V.K. performed the experiments and prepared the main manuscript text. C.K.W. prepared all figures. All authors reviewed and edited the manuscript. D.M.L. and V.V.K. provided financial support.

Data Availability No datasets were generated or analyzed during the current study.

Declarations

Conflict of interest The authors declare no Conflict of interest.

References

1. T. Miyazaki, K.P. Lee, K. Fueki, A. Takeuchi, Temperature effect on the decay of hydrogen (deuterium) atoms in the radiolysis of solid molecular hydrogen, molecular deuterium, and hydrogen-deuterium molecule (HD) at 4.2 and 1.9 K. evidence for tunneling migration. J. Phys. Chem. **88**(21), 4959–4963 (1984). https://doi.org/10.1021/j150665a033
2. K.P. Lee, T. Miyazaki, K. Fueki, K. Gotoh, Rate constant for tunneling reaction $D_2 + D \rightarrow D + D_2$ in radiolysis of molecular deuterium-hydrogen deuteride mixtures at 4.2 and 1.9 K. J. Phys. Chem. **91**(1), 180–182 (1987). https://doi.org/10.1021/j100285a039
3. T. Miyazaki, N. Iwata, K.P. Lee, K. Fueki, Decay of hydrogen(deuterium) atoms in solid hydrogen at 4.2 K: rate constant for tunneling reaction hydrogen (deuterium, hydrogen deuteride) + hydrogen (deuterium) atom. J. Phys. Chem. **93**(8), 3352–3355 (1989). https://doi.org/10.1021/j100345a092
4. E.B. Gordon, A.A. Pel'menev, O.F. Pugachev, V.V. Khmelenko, Hydrogen and deuterium atoms, stabilized by condensation of an atomic beam in superfluid helium. JETP Lett. **37**(5), 282–285 (1983)

5. A.S. Ivliev, A.S. Iskovskikh, A.Y. Katunin, I.I. Lukashevich, V.V. Sklyarevskii, V.V. Suraev, V.V. Filippov, N.I. Fillipov, V.A. Shevtsov, Behavior of hydrogen and deuterium atoms in solid solution of H_2 and D_2 at liquid-helium temperature. JETP Lett. **38**, 317 (1983)
6. H. Tsuruta, T. Miyazaki, K. Fueki, N. Azuma, Remarkable isotope effect on production and decay of D and H atoms in γ-Radiolysis of D_2-H_2 mixtures at 4 K. a quantum-mechanical tunneling effect. J. Phys. Chem. **87**(26), 5422–5425 (1983)
7. S.I. Kiselev, V.V. Khmelenko, D.M. Lee, Hydrogen atoms in impurity-helium solids. Phys. Rev. Lett. **89**, 175301 (2002). https://doi.org/10.1103/PhysRevLett.89.175301
8. T. Kumada, Tunneling chemical reactions D+H_2 →DH+H and D+DH→D_2+H in solid D_2–H_2 and HD–H_2 mixtures: an electron-spin-resonance study. J. Chem. Phys. **124**(9), 094504 (2006). https://doi.org/10.1063/1.2170083
9. S. Sheludiakov, J. Ahokas, J. Järvinen, D. Zvezdov, L. Lehtonen, O. Vainio, S. Vasiliev, D.M. Lee, V.V. Khmelenko, Tunneling chemical exchange reaction D + HD → D_2 + H in solid HD and D_2 at temperatures below 1 K. Phys. Chem. Chem. Phys. **18**, 29600–29606 (2016). https://doi.org/10.1039/C6CP05486B
10. T. Miyazaki, *Atom Tunneling Phenomena in Physics, Chemistry and Biology* (Springer Science & Business Media, 2004). https://doi.org/10.1007/978-3-662-05900-5
11. G.C. Hancock, C.A. Mead, D.G. Truhlar, A.J.C. Varandas, Reaction rates of H(H_2), D(H_2), and H(D_2) van der waals molecules and the threshold behavior of the bimolecular gas-phase rate coefficient. J. Chem. Phys. **91**(6), 3492–3503 (1989). https://doi.org/10.1063/1.456879
12. T. Takayanagi, S. Sato, The bending-corrected-rotating-linear-model calculations of the rate constants for the H+H_2 reaction and its isotopic variants at low temperatures: the effect of Van der Waals well. J. Chem. Phys. **92**(5), 2862–2868 (1990). https://doi.org/10.1063/1.457932
13. T. Takayanagi, N. Masaki, K. Nakamura, M. Okamoto, S. Sato, G.C. Schatz, The rate constants for the H+H_2 reaction and its isotopic analogs at low temperatures: wigner threshold law behavior. J. Chem. Phys. **86**(11), 6133–6139 (1987). https://doi.org/10.1063/1.452453
14. Y. Kagan, L.A. Maksimov, Quantum diffusion in irregular crystals. Sov. JETP **84**, 792–810 (1983)
15. P.C. Stancil, S. Lepp, A. Dalgarno, The deuterium chemistry of the early universe. Astrophys. J. **509**(1), 1 (1998). https://doi.org/10.1086/306473
16. D. Galli, F. Palla, Deuterium chemistry in the primordial gas. Planet. Space Sci. **50**(12), 1197–1204 (2002). https://doi.org/10.1016/S0032-0633(02)00083-1. (**Special issue on Deuterium in the Universe**)
17. C.D. Gay, P.C. Stancil, S. Lepp, A. Dalgarno, The highly deuterated chemistry of the early universe. Astrophys. J. **737**(1), 44 (2011). https://doi.org/10.1088/0004-637X/737/1/44
18. C. Luo, Y. Tan, S. Li, Z. Lu, Y. Shu, W. Chen, D. Yuan, X. Yang, X. Wang, Crossed molecular beam study of the H + HD → H_2 + D reaction at 0.60 and 1.26 eV using the near-threshold ionization velocity map ion imaging. J. Phys. Chem. A **126**(27), 4444–4450 (2022). https://doi.org/10.1021/acs.jpca.2c03296
19. R. Goetting, J.P. Toennies, M. Vodegel, Molecular beam scattering studies of the reaction D + H_2 (v = 0) and D + H_2 (v = 1) → HD + H. Int. J. Chem. Kinet. **18**(9), 949–959 (1985). https://doi.org/10.1002/kin.550180906
20. M.A. Walker, A snowflake's chance in heaven. Mon. Not. R. Astron. Soc. **434**(4), 2814–2824 (2013). https://doi.org/10.1093/mnras/stt1157
21. K.A. Haupa, P.R. Joshi, Y.-P. Lee, Hydrogen-atom tunneling reactions in solid para-hydrogen and their applications to astrochemistry. J. Chin. Chem. Soc. **69**(8), 1159–1173 (2022). https://doi.org/10.1002/jccs.202200210
22. I. Weber, P.R. Joshi, D.T. Anderson, Y.-P. Lee, Unique applications of para-hydrogen matrix isolation to spectroscopy and astrochemistry. J. Phys. Chem. Lett. **15**(45), 11361–11373 (2024). https://doi.org/10.1021/acs.jpclett.4c02733
23. A.V. Ivliev, A.Y. Katunin, I.I. Lukashevich, V.V. Sklyarevskii, V.V. Suraev, V.V. Filippov, N.I. Fillipov, V.A. Shevtsov, Temperature dependence of quantum diffusion of H atoms in solid H_2 in the temperature range 1.35 K ≤ T ≤ 4.2 K. JETP Lett. **34**, 357 (1982)
24. A.S. Iskovskikh, A.Y. Katunin, I.I. Lukashevich, V.V. Sklyarevskii, V.V. Suraev, V.V. Filippov, N.I. Filippov, V.A. Shevtsov, Recombination and spin relaxation of hydrogen and deuterium atoms in molecular crystals. Sov. Phys. JETP **64**, 1085 (1986)
25. J. Ahokas, J. Järvinen, V.V. Khmelenko, D.M. Lee, S. Vasiliev, Exotic behavior of hydrogen atoms in solid H_2 at temperatures below 1 K. Phys. Rev. Lett. **97**, 095301 (2006). https://doi.org/10.1103/PhysRevLett.97.095301

26. J. Ahokas, O. Vainio, J. Järvinen, V.V. Khmelenko, D.M. Lee, S. Vasiliev, Stabilization of high-density atomic hydrogen in H_2 films at T < 0.5 K. Phys. Rev. B **79**, 220505 (2009). https://doi.org/10.1103/PhysRevB.79.220505
27. J. Ahokas, O. Vainio, S. Novotny, J. Järvinen, V.V. Khmelenko, D.M. Lee, S. Vasiliev, Magnetic resonance study of H atoms in thin films of H_2 at temperatures below 1 K. Phys. Rev. B **81**, 104516 (2010). https://doi.org/10.1103/PhysRevB.81.104516
28. S. Sheludiakov, D.M. Lee, V.V. Khmelenko, J. Järvinen, J. Ahokas, S. Vasiliev, Purely spatial quantum diffusion of H atoms in solid H_2 at temperatures below 1 K. Phys. Rev. Lett. **126**, 195301 (2021). https://doi.org/10.1103/PhysRevLett.126.195301
29. S. Sheludiakov, D.M. Lee, V.V. Khmelenko, J. Järvinen, J. Ahokas, S. Vasiliev, Experimental cell with a Fabry-Pérot resonator tuned in situ for magnetic resonance studies of matrix-isolated radicals at temperatures below 1 K. Rev. Sci. Instrum. **91**(6), 063901 (2020). https://doi.org/10.1063/5.0012178
30. S. Sheludiakov, J. Ahokas, J. Järvinen, D. Zvezdov, O. Vainio, L. Lehtonen, S. Vasiliev, S. Mao, V.V. Khmelenko, D.M. Lee, Dynamic nuclear polarization of high-density atomic hydrogen in solid mixtures of molecular hydrogen isotopes. Phys. Rev. Lett. **113**, 265303 (2014). https://doi.org/10.1103/PhysRevLett.113.265303
31. S. Vasilyev, J. Järvinen, E. Tjukanoff, A. Kharitonov, S. Jaakkola, Cryogenic 2 mm wave electron spin resonance spectrometer with application to atomic hydrogen gas below 100 mK. Rev. Sci. Instrum. **75**(1), 94–98 (2004). https://doi.org/10.1063/1.1633006
32. I.F. Silvera, The solid molecular hydrogens in the condensed phase: fundamentals and static properties. Rev. Mod. Phys. **52**, 393–452 (1980). https://doi.org/10.1103/RevModPhys.52.393
33. T. Miyazaki, H. Morikita, K. Fueki, T. Hiraku, Trapping sites of hydrogen atoms in solid hydrogen at 4.2 K analyzed by ESR linewidths. Chem. Phys. Lett. **182**(1), 35–38 (1991). https://doi.org/10.1016/0009-2614(91)80099-J
34. H.D. Megaw, F. Simon, Density and compressibility of solid hydrogen and deuterium at 4.2° K. Nature **138**(3484), 244–244 (1936). https://doi.org/10.1038/138244a0
35. V.V. Khmelenko, E.P. Bernard, S. Vasiliev, D.M. Lee, Tunneling chemical reactions of hydrogen isotopes in quantum solids. Rus. Chem. Rev. **76**, 1107 (2007)
36. S. Sheludiakov, D.M. Lee, V.V. Khmelenko, Y.A. Dmitriev, J. Järvinen, J. Ahokas, S. Vasiliev, Purely spatial diffusion of H atoms in solid normal- and para-hydrogen films. Phys. Rev. B **105**, 144102 (2022). https://doi.org/10.1103/PhysRevB.105.144102